Mansoura Engineering Journal

Volume 35 | Issue 3 Article 7

11-23-2020

Experimental Investigation of Flow Field Characteristics behind V-Shaped Bluff Bodies.

Atef Alam El-Din
Mech. Power Eng., Faculty of Engineering, Port-Said University, & Vice President of Port Said University.

Gamal Moustafa
Mech. Power Dept., Faculty of Engineering, Port Said University., eGYPT

Mohammed Bakr
Mech. Power Dept., Faculty of Engineering, Port Said University.

EXPERIMENTAL INVESTIGATION OF FLOW FIELD CHARACTERISTICS BEHIND V-SHAPED BLUFF BODIES

دراسة عملية لخصائص السريان خلف أجسام على شكل حرف V

Atef M. Alam El-Din *, Gamal H. Moustafa **, Mohammed A. Bakr ***

* Professor of Mech. Power Eng., Faculty of Engineering, Port-Said University, & Vice President of Port Said University.

**Ass. professor Mech. Power Dept., Faculty of Engineering, Port Said University.

***Administrator Mech. Power Dept., Faculty of Engineering, Port Said University.

يتناول البحث دراسة معملية عن سريان الهواء حول أجسام على شكل حرف V لما لها من اهمية كبيرة فى مجالات مختلفة وخصوصا فى مجال الاحتراق حيث يمكن استخدامها كمثبتات للهب بغرض تحسين استقراره. تتكون منطقة دوامات خلف الجسم عند سريان الهواء عليه وهذه الدوامات تحسن من الخلط بين الهواء والغاز فى عملية الاحتراق مما ينتج عنه زيادة استقرار اللهب. تم استخدام نفق هوائى لدراسة سريان الهواء حول جسم واحد عند سرعات هواء مختلفة وكذلك عند زوايا مختلفة لرأس الجسم وكذلك عند زوايا مختلفة لدخول الهواء على الجسم حيث درسنا أثر هذه المتغيرات على توزيع الضغط على سطح الجسم وكذلك على منطقة الدوامات خلف الجسم. أظهرت النتائج انه مع زيادة سرعة الهواء يزداد الضغط على سطح الجسم وتقل حجم منطقة الدوامات خلف الجسم ومع زيادة زاوية رأس الجسم يزداد الضغط على سطح الجسم ماعدا عند نقطة رأس الجسم ويزداد حجم منطقة الدوامات خلف الجسم. وعند تغيير زاوية دخول الهواء على الجسم (زاوية الهجوم) فان سطحى الجسم (الجناحين) أحدهما يقع تحت ضغط موجب والسطح الاخر يحدث عليه تفريغ بينما تتحرك منطقة الدوامات قليلا فى الاتجاه الرأسى الى أعلى او الى أسفل حسب اتجاه زاوية دخول الهواء على الجسم. اضافة لما تقدم تم دراسة السريان حول جسمين وضعا خلف بعضهما فى مستوى واحد مع تغيير المسافة بينهما فأظهرت النتائج انه كلما زادت المسافة بين الجسمين زاد حجم منطقة الدوامات خلف الجسم الثانى. وعندما تم وضع الجسمين فوق بعضهما فى نفس المستوى الرأسى وقمنا بدراسة تأثير تغيير المسافة بين الجسمين على توزيع الضغط على سطحهما ظهر هناك تأثير متبادل وهذا التأثير يقل مع زيادة المسافة بين الجسمين وبالنسبة لمنطقة الدوامات خلف الجسمين وضح انه كلما قلت المسافة بين الجسمين كلما تمت عملية الخلط بين منطقتى الدوامات مبكرا مما يعنى تحسن عملية الخلط بين منطقتى الدوامات لكل جسم.

Abstract

Flow features and vortex shedding in the wake zone behind V-shaped bluff bodies are experimentally investigated. These experiments were done for a single V-shaped body at various Reynolds number between 4.84×10^4 – 5.91×10^4, span angles between 45°-90°,and angles of attack between 0° and 15°. Experiments were also made for two V-shaped bluff bodies arranged in tandem and in the same vertical plane with different spaces between them. With the aid of a water tunnel, the phenomena of vortex shedding and flow recirculation behind the V-shaped bluff body were illustrated. Results show that the increase of Reynolds number monotonically reduces the length of the recirculation zone. A similar flow structure of the flow exists among near wake flows of V-shaped bodies with different span angles. Increasing the span angle, the size of the recirculation zone increases. The variation in attack angle changes slightly the size of the recirculation zone and shifts the recirculation zone vertically. For the two bodies arranged in tandem, the size of the recirculation zone increases as increasing the spacing between the two V-shaped bodies. For the two bodies in the same vertical plane, decreasing the spacing between the two bodies yields to earlier mixing between the flows in the two wakes.

Accepted September 30, 2010.

Introduction

Flow over bluff-bodies has a great importance in the field of Fluid Mechanics as this type of flow is associated with some complicated phenomenons such as boundary layer separation, recirculation, drag force, lift force and shear layers. This type of flow has attracted a lot of researchers in order to explain the flow and its associated phenomenons. Although the effect of wind in producing vibrations in wires (Aeolian tones) had been known for some time, the first experimental observations are due to Strouhal [1], who showed that the frequency depends on the relative air velocity and not on the elastic properties of the wires. After Strouhal there were many researchers that began to study the complicated phenomenons associated to flow over bluff bodies. In 1911, Von Karman gave his famous theory of the vortex street [2], stimulating a widespread and lasting series of investigations of the subject. Roshko [3] used a hot wire anemometer and a pitot tube in investigating the flow past a circular cylinder at Reynolds numbers from 40 to 10,000. Liendhard, [4] studied the different flow regimes past a circular cylinder. He found that at very low Reynolds number, $Re \leq 1.0$, there is no flow separation. As the Reynolds number is increased, there is a flow separation and eddies start to form. Other investigators such as Perry [5] and Coutanceau [6] also gave phenomenological describes on vortex shedding process behind two dimensional bluff bodies. Unal and Rockwell [7] used a water channel in exploring the wake flow with Reynolds number less than 5000. Good quality photographs of the wake flow pattern at low Reynolds number were obtained. Schetz [8] investigated the flow behind a bluff body. He divided the wake into two regions. The first one is the near wake directly behind a bluff body. It is a very complex region. The feature of this area is governed by the shape of the body. The second is the region far downstream from a body while is called the similarity region. In this region analysis is easier because the wake profile is fully developed. The flow over V-shaped bluff bodies is very important as it is used as flame stabilizers. The researches on the V-shaped bluff bodies are little compared with the other shapes of bluff bodies. The V-shaped bluff bodies are also used in many applications, Military airplanes industries as the Delta wings are V-shaped bluff bodies. In marine ships designs as the most of the ships have V-shaped sterns. It is also used in vortex shedding flow meters. The most important application for the V-shaped bluff bodies are their usage as flame holders in the flame stabilizing process. They are usually adopted in many of the combustion apparatuses (e.g., the ramjet combustors, thrust augmenters, industrial burners, turbojet or turbofan afterburners in military aircraft, and rocket motors etc.). This is due to its effective flame-holding ability and low pressure-loss characteristics. They are also employed for

supplementary firing in industrial boilers and heat recovery steam generators. Most of our present understanding of the flame stabilization process is due to the pioneering studies carried out in the 1950's by Zukowski and Marble [9], Cheng and Kovitz [10], Longwell et al. [11], Jensen and Shipman [12] and Williams and Shipman [13]. These studies found that the wake behind the bluff body can be divided into the re-circulation zone and the mixing zone that keeps the re-circulation zone away from the unburned reactants. A very important investigation was made by Jumell et al. [14]. They made a three dimensional preliminary study on the flow over a wedge-shaped bluff body. Fujii et al. [15,16] used a hot wire anemometer and a one-color LDA to study the anisotropic turbulent flow structure of a wedge at low velocities. Yang et al. [17] investigated the mechanism of vortex shedding and turbulent flow characteristics of the near-wake flow behind regular/irregular V-shaped bluff bodies. The influence of the angle of attack and span angle on turbulent flow features at various airflow speeds were given. They found that the length of recirculation zone is linearly decreased with an increase of Reynolds number. There was a similarity among wake flows behind V-shaped bluff bodies with different span angles. The normalized length of recirculation zone stayed constant as span angle varies from 30 to 50 deg. Also, they found that the variation of angle of attack may shift the recirculation zone to a certain vertical distance and slightly change the size of the recirculation zone. Scott et al. [18] used particle image velocimetry (PIV) measurements to determine the flow field around a confined V-shaped bluff body. Rong et al.[19] investigated the oscillating behaviors and frequency of the unsteady flows in the wake of a V-shaped body experimentally using the smoke-wire flow visualization technique. They observed two types of instabilities: the shear-layer instability waves evolving from trailing edges of the wings of V-shaped body and the alternative vortex shedding in the wake.

In the present paper, an experimental work has been done to study the characteristics of the flow behind the V-shaped bluff bodies. The effect of the initial flow Reynolds number, span angle and flow angle of attack are reported. Also, the effect of intermediate distance between two V-shaped bluff bodies placed side by side in a vertical plane or in tandem is studied. Flow visualization is given to identify the flow features.

Experimental Set-Up

Experiments were conducted in an open-circuit wind tunnel (see Fig. 1). A uniform air stream was supplied to the test section by two similar centrifugal air blowers 7.5 hp each. A system of speed control was attached in which the speed of the two blowers was regulated by

an AC inverter manufactured by Toshiba Company (model VF-S11). Therefore, the air mass flow rate was controlled according to the experimental requirements. The maximum flow rate provided by the two blowers was 50 m^3/min at a static pressure difference of 7000 mm H_2O. The dimensions of the test section was 30 cm × 30 cm cross section and 100 cm length. The test section was fabricated with one side of glass, Fig.(2). This glass side could be easily removed and fastened in order to fix and change the test models. The upper side of the test section was arranged to fix the traverse system. A two dimensional traversing system of 1.5 mm pitch in the x and y directions was used to control the Pitot probe movement. The test models were made of wood and were polished to be smooth. The wall static pressure distributions on the two wings of the V-shaped bodies were measured through 7 tapes of 0.5 mm inner diameter connected to a multi U tube water manometer. The pressure and velocity measurements in the recirculation zone were made by using a well calibrated five holes Pitot probe and a software program. Details of the tested V-shaped bodies is shown in Fig.(3).

The initial speed was varied from 31.56 m/sec to 38.55 m/sec. Hence the Reynolds number based on d (blockage width) was ranged from 4.84×10^4 to 5.91×10^4. The span angle (β) was chosen as 45°, 60°, 75°, 90°. Experiments were done for attack angle (α) ranging from 5° to 15°.

For the arrangements of two V-shaped bodies, experiments were made at $\beta = 45°$, $\alpha = 0°$, $Re = 5.2 \times 10^4$ with different intermediate spaces.

Uncertainty of 5-holes probe measurements

Velocity measurements are subject to errors in particular in reversed flow regions. The other parameters recorded during the experimental runs and the respective measurement uncertainties are listed in the below table.

Table 2 The accuracy limits for the measured parameters.

Parameter	Accuracy limit
Barometric pressure	± 0.1 mm Hg
Probe angle	± 2°
Air density, ρ	± 5 %
Inlet air temperature	± 0.5 °C
Dynamic viscosity, μ	± 3 %

The precision limits seen in the table are the smallest interval between the scale markings (least count) of the perspective instruments. The bias limit for instruments was negligible. An error analysis including the effects of both bias and precision errors, using the root-sum-square method, showed that the uncertainty in the measured mean velocity (u) is ± 4.8 % within 95 % confidence. Other uncertainty values are summarized below.

Table 3 Estimated typical uncertainties

Parameter	U %
u	± 4.8
p	± 6.83
v, w	± 5.2

Results and discussion

The pressure and the velocity at the entrance of the test section were measured by the five holes probe to be used as a reference values (see below table).

Table 1 Pressure and Velocity reference values

Re. No.× 10^{-4}	5.91	5.61	5.21	4.84
C_{ref} (m/sec)	38.55	36.60	34.00	31.56
$P_{ref\,g}$ (N/m^2)	862.4	754.6	695.8	637.0

The wall pressure distribution along the upper and lower surfaces of the V-shaped body at different Reynolds numbers is given in Fig.4. It is seen that the pressure distribution indicates a very interesting phenomenon in which it has the same shape of the V-shaped body. The wall pressure is a maximum at the stagnation point (the nose of the V-shaped body). It decreases as the flow moves downstream. The flow angle of attack is zero and the flow pattern shows symmetrical features along the upper and lower surfaces of the V-shaped body. It is seen that as the Reynolds number increases the wall pressure at all points is increased.

In Fig.5, the wall pressure distribution is given for different span angles and zero angle of attack. It is found that the maximum pressure is recorded at the stagnation point. The wall pressure decreases gradually as the flow moves downstream. The pressure distribution have the same pattern for all span angles as it has the same shape of the V-shaped body. It was noticed that as the span angle increases, there is a slight increase in the wall pressure at all measuring tapes except tape No. 0 has a constant pressure value and this is logic as, if the span angle increased to 180°, the pressure at the measuring tapes will be go close to the stagnation pressure.

The effect of the flow angle of attack on the flow feature is given in Fig.6 for Re = 5.91 × 10^4 and span angle = 45°. Symmetrical features are shown for zero angle of attack. The maximum pressure shifts from the pressure measuring tape No. 0 to the upper or lower surfaces of the V-shaped body according to the direction of the attack angle. The side faces the flow is called the pressure side in which the pressure values at the three measuring points are positive. The other side is called the suction side, the pressures at the three measuring points are negative. It is seen that increasing the attack angle the location for maximum pressure moves downstream on the surface and the magnitude of the pressure at all points on the pressure side increases while the pressure at all points on the suction side decreases.

For the two V-shaped bodies placed in tandem there is an interesting feature. The second body is immersed in the wake region of the first body. The wall pressure distribution for the back body is given in Fig.7. The pressure distribution have the same pattern for the three intermediate spaces between the two V-shaped bodies. It has the reversed shape of the V-shaped body. The lowest pressure is sensed by the pressure measuring tape No. 0 as

it located in the eye of the wake zone of the first V-shaped body. For the other measuring tapes the pressure increases gradually as the location of the tapes goes far from the eye of the wake. It is observed that the pressure at all points of the second V-shaped body is decreased by increasing the distance between the two bodies.

For the two V-shaped bodies placed at the same vertical line, the distribution of the wall pressure shows a slight increase at the surfaces of the two wings facing each other; as each body directs part of the flow towards the other body. Therefore, each body affects the other body and this effect decreases with increasing the space between them, Fig.8.

A wake is defined as a deficit of momentum and energy behind a body in a fluid flow [20]. This drop in momentum is evidenced by a decrease in velocity and total pressure. The wake is formed when the flow separates at the trailing edges of the V-shaped body. These separation streamlines form a shear layer between the faster free stream and slower moving fluid. The area within the shear layers is the wake. The two shear layers from each wing of the V-shaped body do not interact until very far downstream. The wake that is formed moves downstream until eventually it dissipates back into the free stream. The flow characteristics in this wake zone have the crucial influence in the flame holding application by improving the mixing between air and fuel. This wake zone consists of high temperature in combustors burnt products that act as a continuous ignition source for the fresh fuel/air mixture.

Fig. 9 indicates the total pressure distributions at different vertical planes in the wake region for a single V-shaped body at $\beta = 45°$, $\alpha = 0°$ and $Re = 5.91\times 10^4$. The pressure distribution is symmetric with respect to P^* axis as the flow attack angle equals zero. There is a pressure variation at every plane. At every plane, X^*, and at the point $Y^*= 0$, the magnitude of the total pressure has a smallest value as it located at the eye of the wake. It increases as goes up or down in the vertical plane (Y direction), reaches the same value of the free stream pressure. The pressure variation is greatest at plane A ($X^* = 0.1667$). As goes down stream (planes B, D, E, F and G) this pressure variation becomes small till a plane where the pressure equal the free stream pressure. At this plane the effect of V-shaped body on the flow field has been finished.

The flow features of the flow field are the same for all Reynolds numbers, However, the length of the wake region is decreased as the Reynolds number is increased, Fig.10. This figure indicates the pressure contours in the wake region. From this figure the wake region could be indicated by the area bounded by the contour line $P^* = 1$ as the pressure is negative inside this area and positive outside it. This pressure contour line meets the X^* axis at $X^*= 3.1$ for Reynolds number $= 5.91\times 10^4$ and at $X^*= 5$ for Reynolds number $= 4.84\times 10^4$

which indicates that the length of the wake region is decreased by increasing the Reynolds number.

Figure 11 indicates the total pressure distribution at the plane X*= 3 in the wake region for various V-shaped bodies at different span angles. It is noticed that the pressure variation is greatest in the case of a V-shaped body with 90° span angle which indicates that the size of the wake region is increases by increasing span angle. This result was confirmed by drawing the total pressure contours for the flow field in the zone behind the V-shaped body at different span angles as given in Fig. 12. It is clear that the length and width of the wake zone increases with increasing the span angle.

Figure 13 shows the pressure distribution in the wake region at different flow angles of attack. The wake slightly shifts vertically as the attack angle is changed.

For the two V-shaped bodies placed in tandem, the pressure distribution in the wake region of the back body has the same pattern at the three intermediate spaces. However the length of the wake region is increased as the intermediate space increased, Fig. 14.

Fig. 15 shows the pressure distribution in the wake region of two geometrically similar V-shaped bodies arranged vertically. By decreasing the intermediate space between the two bodies, the merging process between the two wakes is happened earlier downstream the two bodies. This means that the merging process between the two wakes is enhanced and this will be suitable for flame holding applications.

Fig. 16 shows the absolute velocity distribution in the wake zone for different span angles V-shape bodies at X*= 0.167. It is observed that the absolute velocity distribution have the same pattern like the total pressure distribution.

Conclusion

An experimental work was done to study the flow over a V-shaped body at different initial flow conditions. From the results one can conclude that:-

- Increasing the flow Reynolds number reduces the length of the wake zone and increases the pressure magnitude on the surface of the V-shaped body.
- Increasing the span angle increases the size of the wake zone and increases the pressure magnitude on the V-shaped body surface except at the stagnation point the pressure is the same for all span angles.
- The wake is slightly shifted vertically as the attack angle is increased. Increasing the angle of attack moves the stagnation pressure point on the surface of the V-shaped body and increases the pressure magnitude on the pressure side and reduces the pressure magnitude on the suction side.

- Increasing the space between the two V-shaped bodies arranged in tandem increases the length of the wake zone and increases the pressure magnitude on the surface of the back body.
- For the two V-shaped bodies arranged vertically, as the space decreases, the two wakes merge at earlier axial distances and the distribution of the magnitude of wall static pressure is affected by the distance between the two bodies.

Nomenclatures

- Re Reynolds Number $Re = \frac{\rho \times Cref \times d}{\mu}$
- μ Air dynamic viscosity = 1.8×10^{-5} N.s / m^2 (at T = 20°C)
- ρ Air density 1.2 Kg/ m^3 at T=20°C
- L Length of the wing of the V-shaped body
- d Blockage width of V-shaped body
- β Span angle of V-shaped body
- α Angle of attack
- C Absolute velocity
- P^* = (Pt + Patm)/ Patm
- P_{atm} Atmospheric pressure
- P_i Measured pressure
- Cp_i $=(P_i - P_{ref}) / (0.5 \rho C_{ref}^2)$
- P_{ref} Reference pressure
- C_{ref} Reference velocity
- C^* $= C/C_{ref}$
- S_h^* $= S_h / L$
- S_h = Distance between bodies in tandem
- S_v^* $= S_v / L$
- S_v =Distance between bodies arranged vertically
- X^* $= X / L$
- Y^* $= Y / L$
- Z^* $= Z / L$

Refrences

[1] Strouhal, V., "Ueber eine besondere Art der Tonerregung", Ann. Phys. und Chemie, Neue Folge, Bd. 5, Heft 10, Oct. 1978, pp. 216-251.

[2] Von Karman, Th., and Rubach, H., "Ueber den Mechanismus des Flussigkeits und

Widerstandes" Phys. Zs., Bd. 13, Heft 2, Jan. 15, 1911, pp. 49-59.

[3]Roshko, A., "On the Wake and Drag of Bluff Bodies" Journal of the Aerospace Sciences, Vol. 22, Feb. 1955, pp. 124–135.

[4] Liendhard, J., H., *"Synopsis of Lift, Drag, and Vortex Frequency Data for Rigid, Circular Cylinders"* Washington State University, Research Division Bulletin 300, 1966.

[5] Perry, A., E., "The Vortex Shedding Process Behind Two-Dimensional Bluff Bodies" J Fluid Mech 1982;116: pp. 77–90.

[6] Coutanceau M., D., "On the role of high Order Separation on the Onset of the Secondary Instability of the Circular Cylinder Wake Boundary" Academie des Sciences (Paris), Comptes Rendus, Serie II – Mecanique, Physique, Chimic, Science de la Terre (ISSN 0249- 6305), vol. 306 No. 18 May 14, 1988, pp. 1259- 1263

[7] Unal M., F., Rockwell D., A., "On Vortex Formation from a Cylinder" J Fluid Mech 1988;199: pp.491–512.

[8] Schetz, J., A., "Foundations of Boundary Layer Theory for Momentum" Heat and Mass Transfer, Prentice Hall, 1984, pp. 220-254.

[9] Zukowski, E., E., and Marble, F., E., "The Role of Wake Transition in the Process of Flame Stabilization in the Bluff Bodies," AGARD Combustion Researches and Reviews, Butterworth Scientific Publishers, London, 1954, pp. 167-180.

[10] Cheng, S., I., and Kovitz, A., A., "Theory of Flame stabilization by a Bluff body," Proc. Comb. Inst., Vol. 7, 1958, pp. 681-691.

[11] Longwell, J., P., Chenevcy, J., Clark, W., and Frost, E., "Flame Stabilization by Baffles in a High Velocity Gas Stream," Proc. Comb. Inst., Vol. 3, 1951, pp. 40-44.

[12] Jensen, W., P., and Shipman, C., W., "Stabilization of Flames in High Speed Flows By Pilot Flames," Proc. Comb. Inst., Vol. 7, 1958, pp. 674-680.

[13] Williams, G., C., and Shipman, C., W., "Some Properties of Rod Stabilized Flames of Homogeneous Gas Mixtures," Proc. Comb. Inst., Vol. 4, 1953, pp. 733-742.

[14] Jumel, J., O., King, P., S., and Brien, W.,F., "Transient Total Pressure Distortion Generator Development" Final Report for Academic Qualification, Blacksburg, VA, July, 1999.

[15] Fujii, S., and Eguchi, K., "A Comparison of Cold and Reacting Flows around a Bluff Body Flame Stablizer" Journal of Fluids Engineering Vol 103 No. 2 1981, pp.328-334.

[16] Fujii, S., Gomi, M., and Eguchi, K., "Cold Flow Tests of a Bluff Body Flame Stabilizer," Journal of Fluids Engineering, Vol. 100, Sept. 1978, pp. 323-332.

[17] Yang, J., Tsai, G., and Wang, W., "Near-Wake Characteristics of Various V-Shaped Bluff Bodies" Journal of Propulsion and Power Vol. 10, Jan-Feb 1994, pp. 47-55.

[18] Scott, M., Bush, and Ephraim, J., Gutmark, "Reacting and Non-Reacting Flow Fields of a V-gutter Stabilized Flame" 44th AIAA Aerospace Sciences Meeting and Exhibit 9-12 January 2006, Reno, Nevada.

[19] Rong, F., Huang, and Kuo, T., Chang, "Oscillation Frequency in Wake of a Vee Gutter" Journal of Propulsion and Power - Vol. 20, No. 5, September–October 2004.

[20] Belvins, R.D., "Applied fluid dynamics handbook", Van Nostrand Reinhold Company, 1984, pp.279-381.

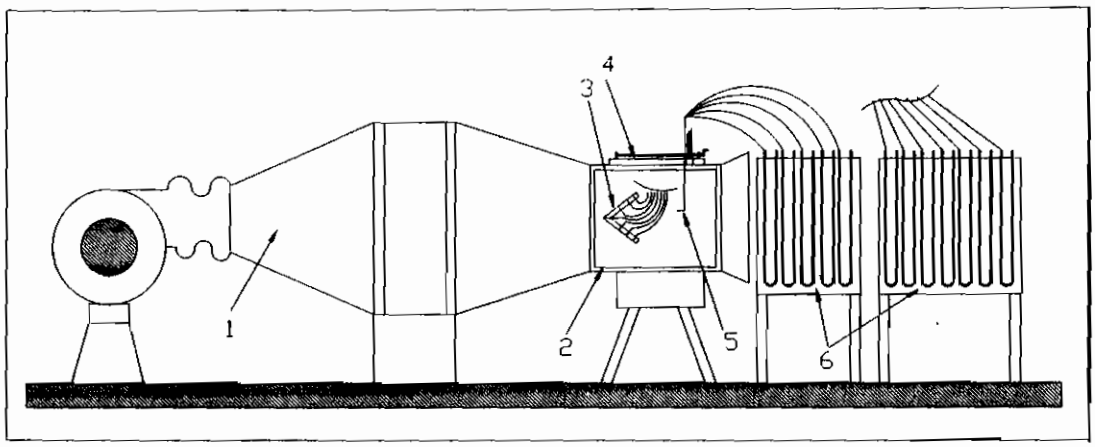

1- Wind tunnel 2- Test section 3- V-shaped body

4- Traversing system 5- Pitot probe 6- U tube manometers

Fig. 1 Experimental test rig.

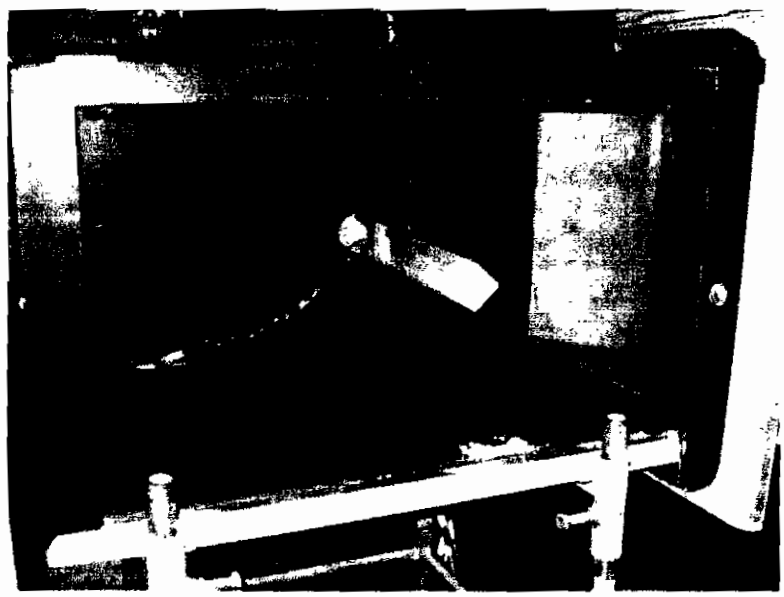

Fig. 2 Test section

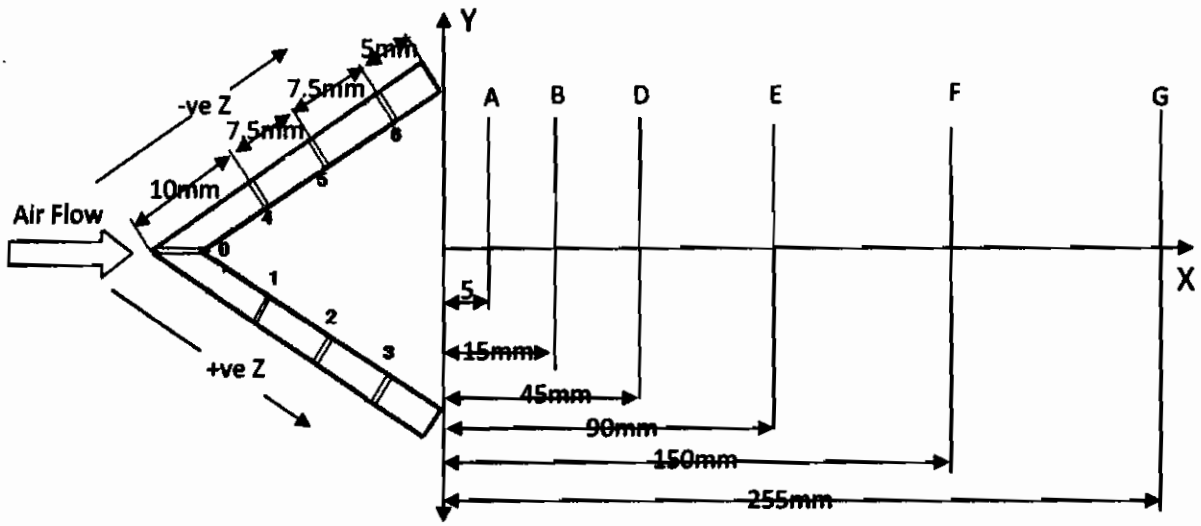

a) Wall pressure measurements tapes and scanned planes in the wake region

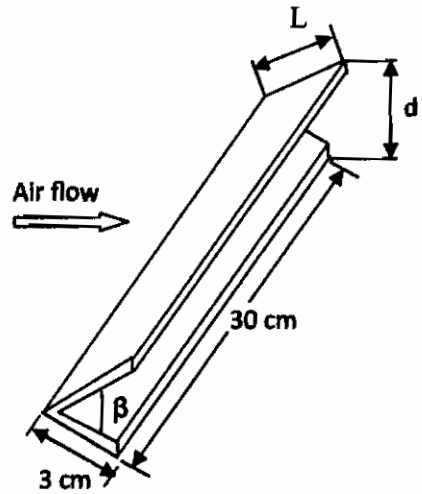

b) V-shaped body dimensions

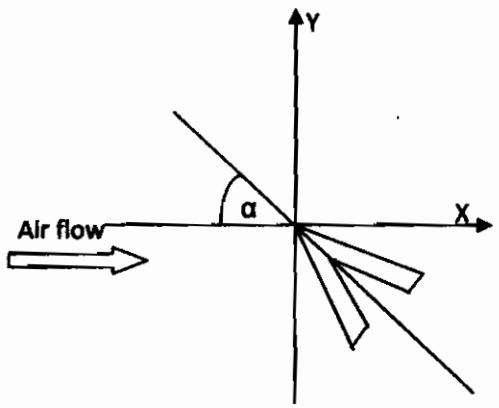

c) Attack angle

Fig.3 Configurations and dimensions of V-shaped bodies

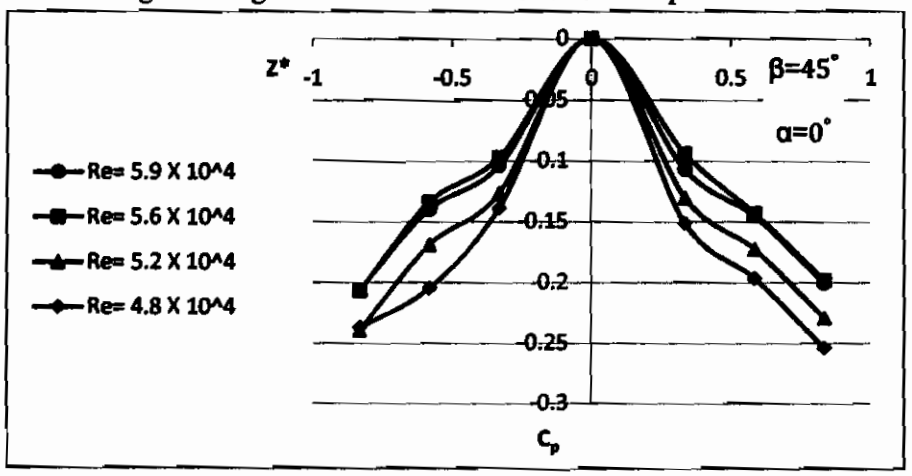

Fig.4 Pressure distribution at various Reynolds numbers

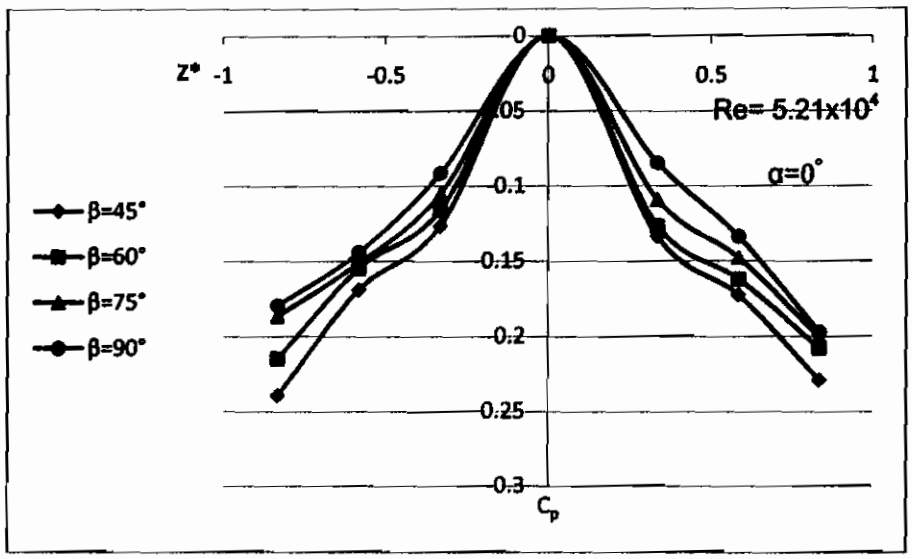

Fig.5 Pressure distribution at various Span angles

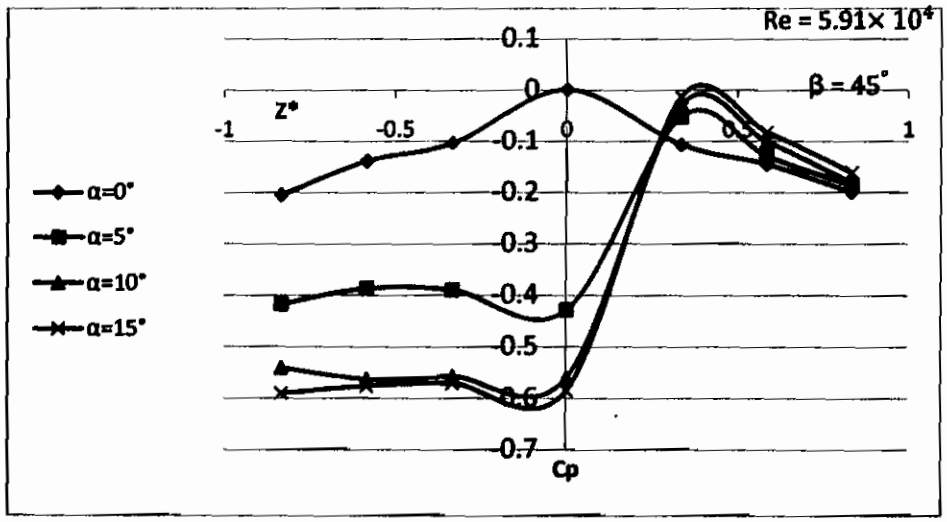

Fig.6 Pressure distribution at various angles of attack

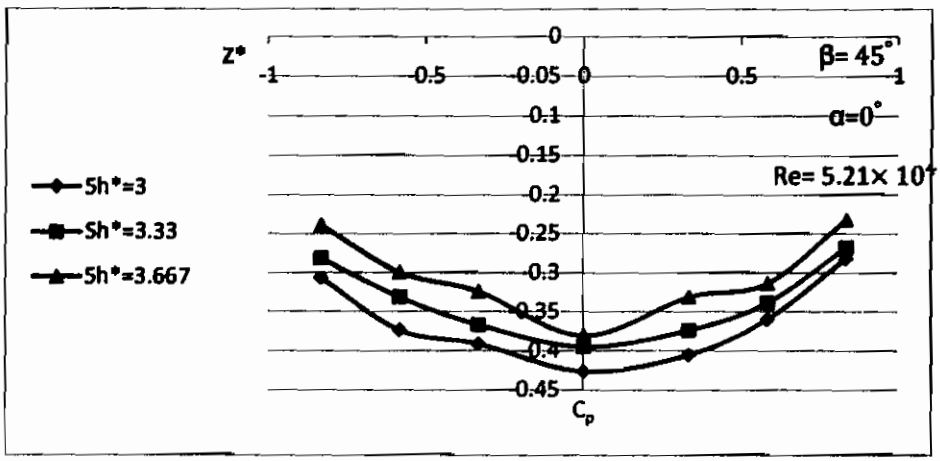

Fig. 7 Pressure distribution (back body) for two bodies in tandem at different spaces.

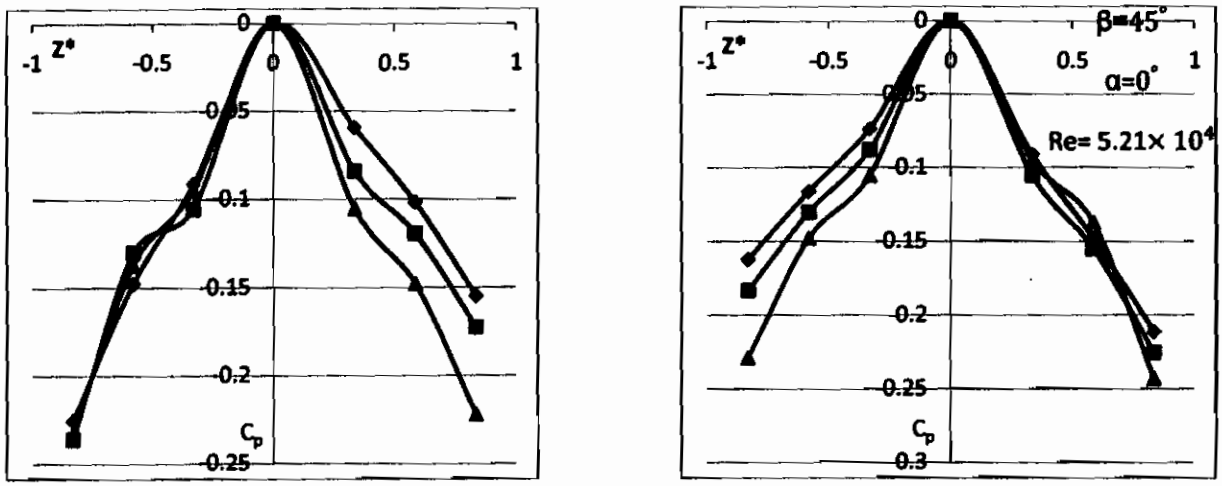

a) Upper body b) Lower body

S_v^*=1 S_v^*=1.33 S_v^*=1.67

Fig. 8 Pressure distribution for two bodies arranged vertically at different spaces

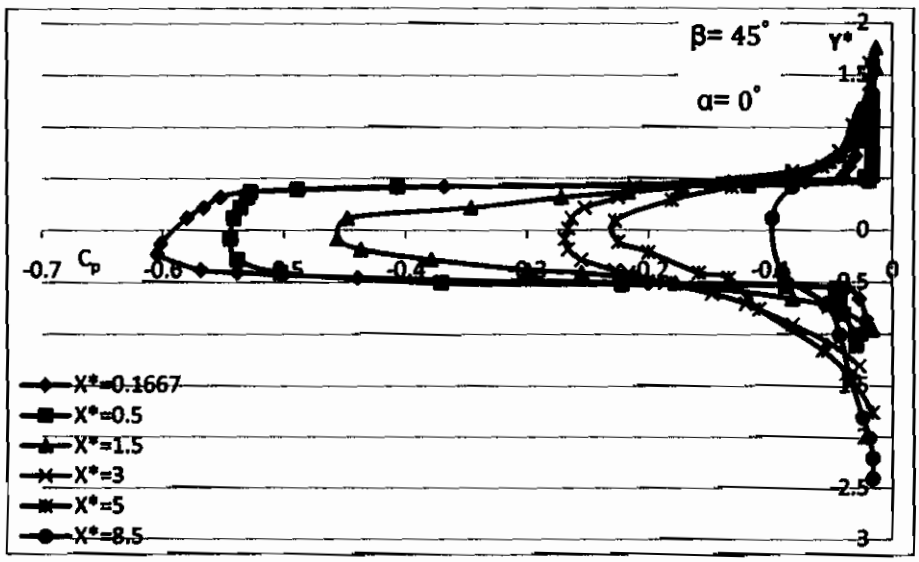

Fig. 9 Total pressure distribution at Re= 5.91× 10^4

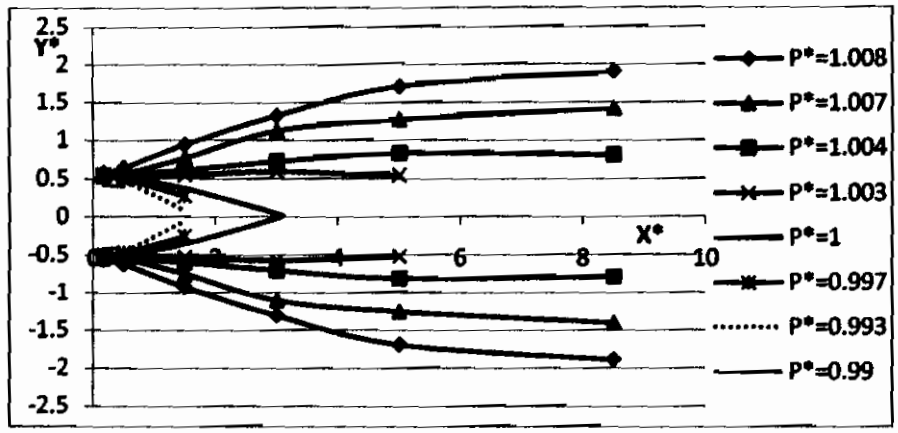

(a) Re = 5.91× 10^4

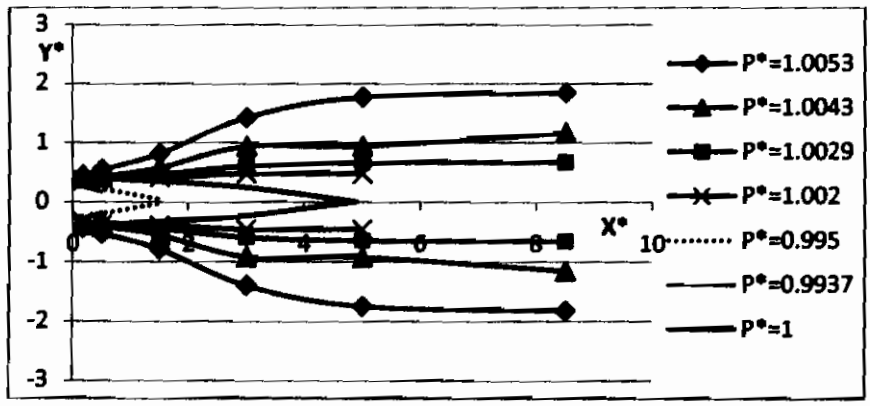

(b) Re = 4.84× 10^4

Fig. 10 Pressure contours in the wake zone of a V-shaped body ($\beta = 45^{\circ}$ &$\alpha = 0^{\circ}$) at different Reynolds numbers.

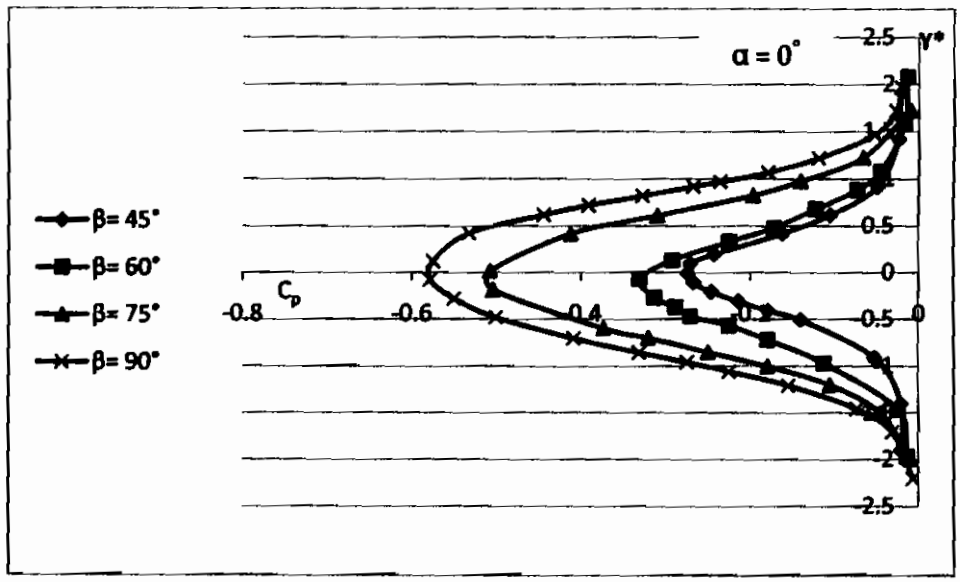

Fig. 11 Pressure distribution for various β at the plane X* = 3

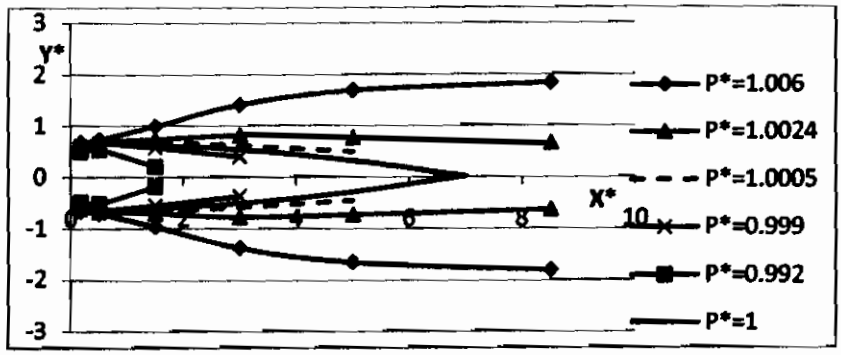

(a) $\beta = 60^{\circ}$

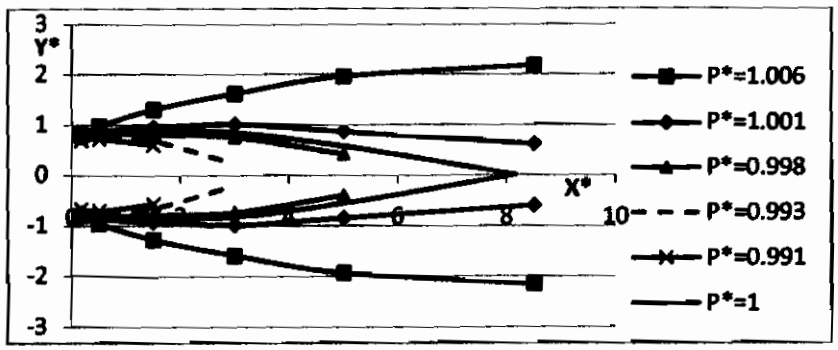

(b) $\beta = 75^{\circ}$

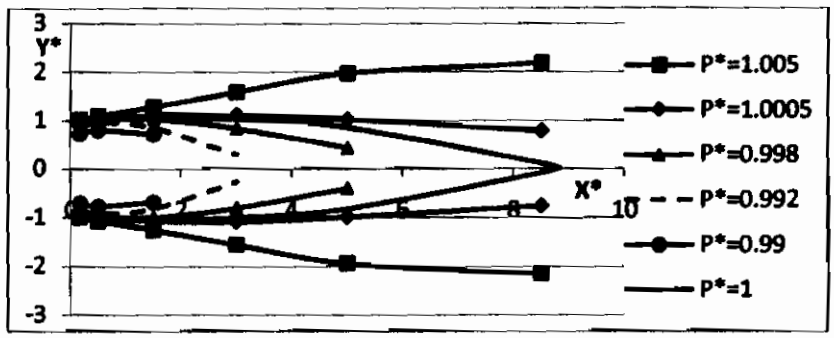

(c) $\beta = 90^{\circ}$

Fig. 12 Pressure contours in the wake zone of a v-shaped body ($\alpha = 0^{\circ}$) at different β

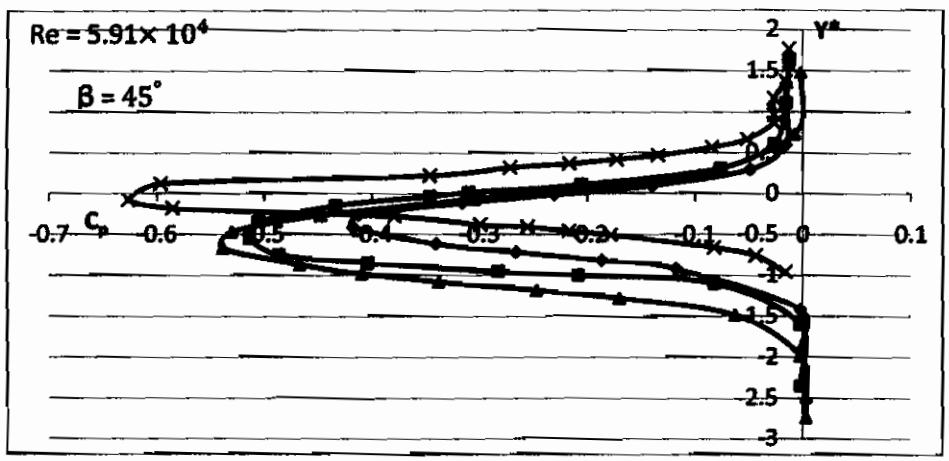

Fig. 13 Pressure distribution for various α at the plane $X^* = 1.5$

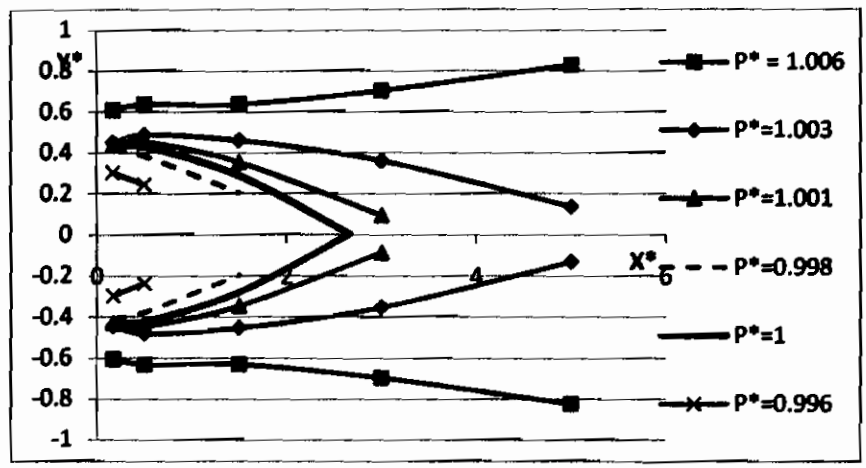

(a) S* = 3

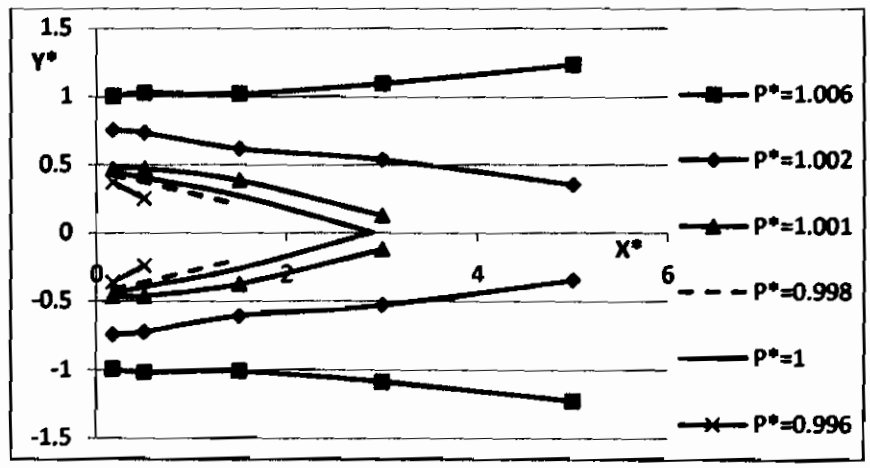

(b) S* = 3.33

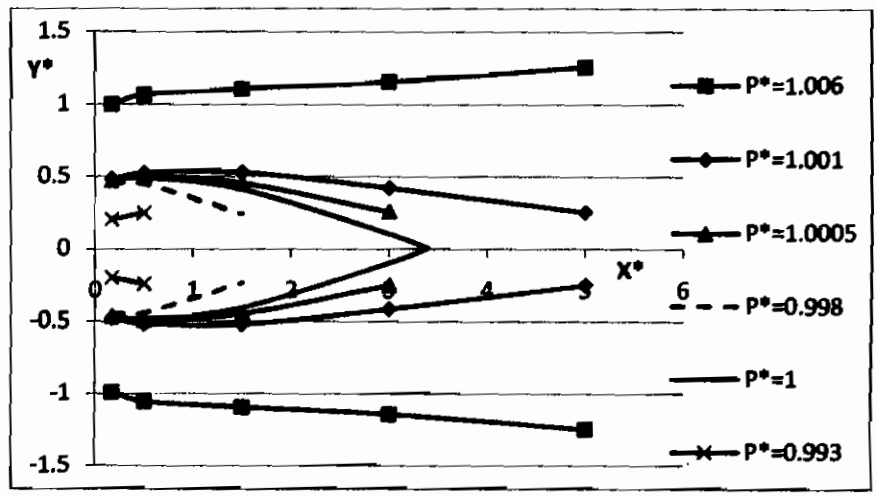

(c) S* = 3.667

Fig. 14 Pressure contours in the wake of the back body of two V-shaped bodies in tandem at different Spaces

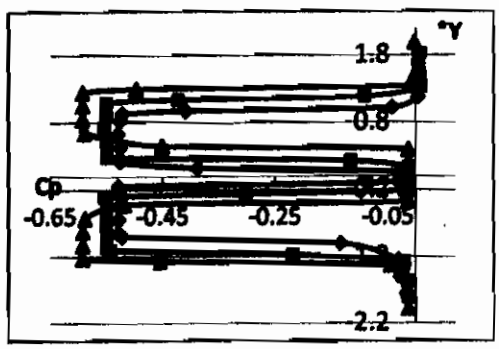

(a) $X^* = 0.1667$

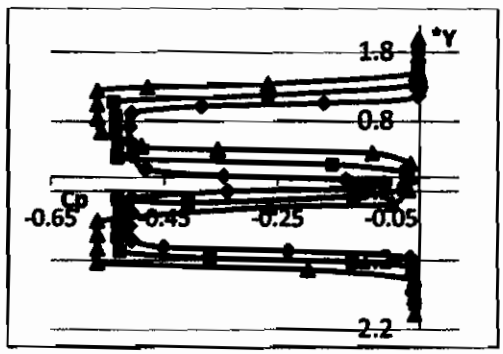

(b) $X^* = 0.5$

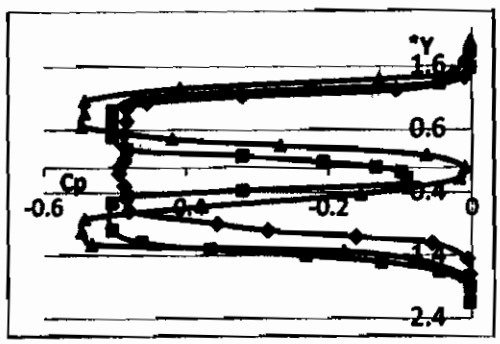

(c) $X^* = 1.5$

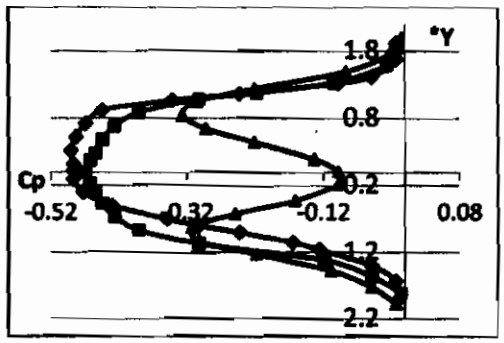

(d) $X^* = 3$

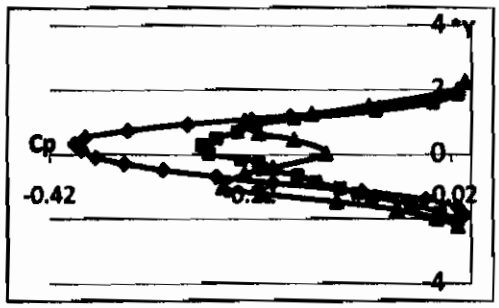

(e) $X^* = 5$

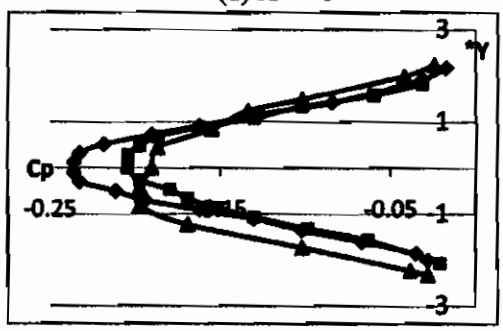

(f) $X^* = 8.5$

$S^* = 1$ $S^* = 1.33$ $S^* = 1.67$

Fig.15 Pressure distribution for two vertically aligned v-shaped bodies at different spaces.

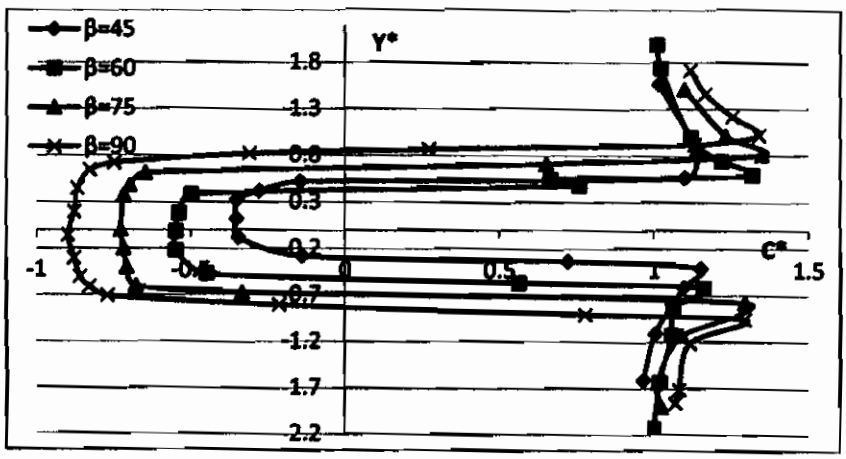

Fig. 16 Absolute velocity distribution for a single body at various β